Fronthaul design for Radio Access Networks using Multicore Fibers

José Manuel Galve, Ivana Gasulla, Salvador Sales and José Capmany

Instituto de Telecomunicaciones y Aplicaciones Multimedia,
Universitat Politècnica de València,
8G Building - access D - Camino de Vera s/n - 46022 Valencia (Spain)
Corresponding author: jcapmany@iteam.upv.es

Abstract

We propose the use of spatial division multiplexing supported by multicore fibers (MCFs) to implement a new generation of flexible and capacity reconfigurable C-RAN front-haul architectures capable of addressing their main present and future challenges. We show that for the majority of radio access scenarios where fronthaul optical links are less than 10-km long, the impact of inter-core crosstalk on the electrical carrier-to-noise ratio can be neglected and, thus, link design can be carried independently core by core. In addition, this MCF-based approach, which is compatible with SDN and NFV, can also support the integration of a passive optical network overlay.

1. Introduction

In converged broadband fiber-wireless access networks, radio services are delivered as an overlay over existing passive optical network (PON) and local ring infrastructures. The typical configuration of a converged or fixed-wireless includes both the wired baseband (BB) and the radio access network (RAN) segments that share a considerable part of common infrastructure [1]. Traditional RANs, are composed of many stand-alone, macro base stations (BTS), which include three different parts [2-5]: the radiating element, usually composed of a three-sector antenna site, a separate cell site cabinet (CSG) that hosts the main equipment of the BS, including the remote radio units (RRU), the baseband unit (BBU), a digital radio over fiber (DRoF) configuration connecting the RRUs to the BBU and the system module. Finally, the cell site gateway (CSG) interfaces the CSC to the backhaul network. In the BTS, the downstream signal received from the central office (CO) through the backhaul network is in baseband format. It is processed by the BBU, up-converted to radio and sent to the three different RRUs by means of three different DRoF links. At the RRUs, the signal is down-converted again to the radio-frequency domain and sent through pairs of RF coaxial cables to the antennas on the BTS tower where it is radiated. The same operations in reversed order are performed for the received up-stream signal.

The traditional RAN architecture has several important drawbacks. First, when more BTSs are added to the system to improve capacity the interference among BTSs is severe as more BTSs are using the same frequency and BTSs are closer to each other. Secondly, each BTSs is costly to build and operate, as it needs a considerable number of autonomous equipment, including its own cooling, back haul transportation, backup battery, monitoring system, etc. Although size and power of the electrical equipment is constantly being reduced, the supporting facilities of the BTS are not improved in the same pace. Finally, because mobile users are moving from one place to another, the traffic managed by each BTS experiences considerable time fluctuations and, as a result, the average utilization rate of individual BTSs is pretty low.

Much of the above limitations can be solved if many of the processing resources can be shared among various BTSs and this has led the evolution towards the so-called centralised RANs (C-RANs) [3]-[5], where the BBUs are hosted in the CO rather than at the remore BTS location. C-RANs need a careful design of its fronthaul segment that is composed of multiple parallel optical fiber connections between the BBUs and the antennas. Furthermore, since 2x2 and 4x4 multiple input multiple output (MIMO) radio transmission from the antenna to the mobile terminals is being considered, the requirement for parallel connectivity between the BBUs and the radiating elements can be increased up by a 4 or 16 factor respectively.

Despite their apparent complexity, the C-RAN concept brings considerable advantages. Amongst them, it is worth mentioning operational and capital expenditure

MCF-CRAN architectures can be flexible enough to support both digital and analog Radio-over-Fiber approaches, allowing software-defined networking and Network function virtualization.

savings, reduced power consumption and improved radio performance derived from the potential low latency between BSs, enabling the possibility of implementing Coordinated Multi-Pont (CoMP) and Long Term Evolution Advanced (LTE-A) systems. C-RANs require the introduction of an optical fronthaul segment for the remote feeding from the CO of different BS Remote Radio Heads (RRHs) and antennas, which may in addition feature (MIMO) radiating elements per sector. Digital Radio-over-Fiber (DRoF) is employed to transport the baseband signal from a given BBU to its corresponding RRH, and vice versa, using one of the protocols defined in the Common Public Radio Interface (CPRI) or the Open Base Station Architecture Initiative (OBSAI).

CRANs face a number of important challenges. The first one is related to bit rate requirements. For instance, CPRI requires very high symmetric bit rates compared to real data rate on the user equipment. For instance, the transport of 5 contiguous 20-MHz LTE-A channels requires a bit rate of 6.144 Gb/s/sector. This figure can grow up to almost 50 Gb/s/sector if the capacity is increased by means of exploiting, for instance, 8x8 MIMO. To solve this limitation some contributions have suggested the direct use of analog Radio over Fiber (RoF) between the BBU and the RRHs [5], [6]. The second challenge is related to fiber availability. In principle, at least 6 fibers are required per 3-sector cell for single antenna operation. If MIMO configurations are targeted, then some kind of multiplexing (such as wavelength division multiplexing (WDM)) must be considered to cope with the constraint of not increasing the fiber count. A third challenge is the need to support other features, such as capacity increase by carrier aggregation, dynamic capacity allocation as well as centralized control, supervision and management. A final challenge resides in its integration in current and/or evolved versions of passive optical access networks (PONs).

In this paper we propose the use of homogeneous multicore fibers (MCFs) to support CRAN architectures capable of meeting the former challenges through the exploitation of spatial division multiplexing (SDM). MCFs are usually available in 7- and 19-core formats [7] and feature negligible crosstalk values (<-50 dB) for links below 10 km, which are currently the 96% of the access networks. We show that homogeneous MCF-CRAN architectures can be flexible enough to support both DRoF and RoF approaches, capacity upgrade by carrier aggregation and MIMO, CoMP operation and true cloud operation. The key advantage brought by this configuration is the fact that, due to the spatial diversity inherent to MCFs, these features can be enabled by means of electronic spatial switching at the CO, thus allowing software defined networking (SDN) and Network function virtualization (NFV). Furthermore, this configuration is compatible and potentially upgradable using WDM and can support as well a PON overlay.

The paper is structured as follows: in section 2 we describe some of the salient features and requirements of C-RANs. In section 3 we describe the main evolutions that CRANs and their associated BTSs have experienced during the last years. Section 4 presents the analog fiber link between the CO and one sector of the BS based on an homogeneous MCF that is the building block of the proposed architecture. It develops some basic link design equations, which must take into account the effect of inter-core crosstalk. It is shown that for most of the practical situations where MCF CO-BS sector links are less than 10-km long the effect of inter-core crosstalk on the electrical carrier to noise ratio (CNR) can be neglected and, therefore, each analog link from the CO to the BS and viceversa can be independently designed. Section 5 investigates the possibility of exploiting the versatility provided by the inherent parallelism of MCF transmission to implement flexible and capacity reconfigurable RAN architectures. Two cases of practical interest are considered, corresponding to pure RoF and DRoF respectively. In each scenario, centralized techniques for capacity reconfiguration are discussed. Section 6 considers the potential integration of PONs in the proposed architectures. Finally in Section 7 we draw up the summary, conclusions and future directions of research.

2. C-RAN Description

Figure 1 shows a typical configuration of a converged or fixed-wireless mutualised access network. It includes both the wired baseband (BB) and the RAN segments that share a considerable part of common infrastructure. In the context of microwave photonics and radio over fiber applications we are mainly interested in the RAN segment.

Traditional RANs, are composed of many stand-alone, all in one, BTSs. Figure 2 shows a typical configuration of one of such BTS.

The structure of a macro BTS includes three different parts: the radiating element, usually composed of a three sector antenna site, a separate CSG that hosts the main equipment of the BS, including the RRU, the BBU, a DRoF configuration connecting the RRUs to the BBU and the system module. Finally, the CSG interfaces the CSC to the backhaul network. Most 1G and 2G BTSs employed this all-in-one architecture, hosting both the analog, digital and power functions in a big CSC, usually placed in a dedicated equipment room with all necessary site supporting facilitates like power, backup battery, air condition, environment surveillance system, backhaul transmission equipment, etc.

In the BTS, the downstream signal received from the central office thorugh the backhaul network is in baseband format. It is processed by the BBU, up-converted to radio and sent to the three different RRU by means of three different DRoF links. At the RRUs, the signal is down-converted again to the radifofrequency domain and sent through pairs of RF coaxial cables to the antennas on the BTS tower where it is radiated. The same operations in reversed order are performed for the received up-stream signal. This all-in-one base station architecture has been mostly employed in macro-cell deployment in 1G and 2G cellular networks, as shown in figure 3. A given BTS covers a small geographical area, while a group of BTSs can provide extended coverage over a continuous area.

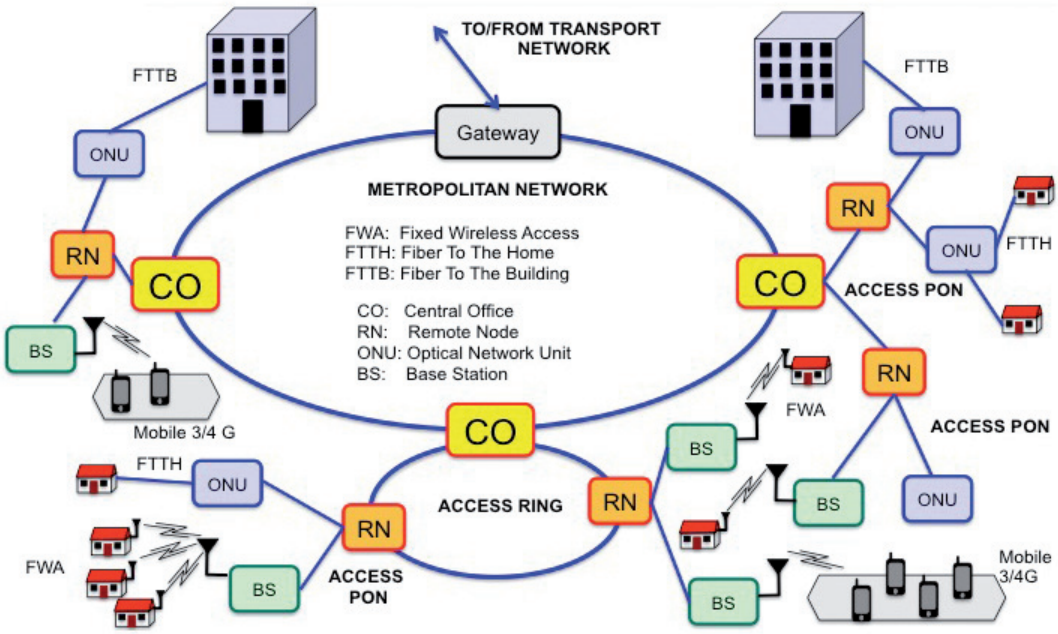

Figure 1. Converged broadband fiber-wireless access network, where radio services are delivered as an overlay over existing passive optical network (PON) and local ring infrastructures.

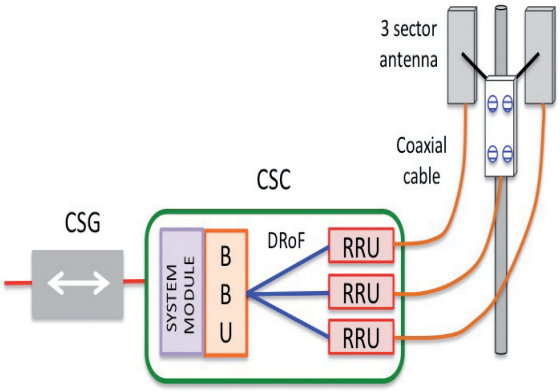

Figure 2. Basic layout of a traditional Macro Base Station.

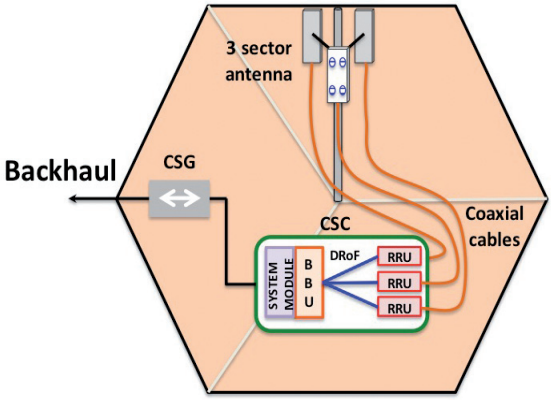

Figure 3. Illustration of the coverage area of a Macro BTS and its backhaul link.

Because of the limited resource of spectrum, cellular networks reuse the available frequencies among the different BTSs. The consequence of this is that neighbouring BTSs that use the same frequencies experience interference in both downlink and uplink transmission directions. Figure 4 shows, as a summary, the typical architecture of a traditional RAN where the backhaul part and the connections to the central office and the transport network are clearly indicated. Note that the backhaul network is ususally composed of a set of point-to-point optical fibre links.

The traditional RAN architecture has some important drawbacks. First, when more BTSs are added to the system to improve capacity, if the same frequency resource is reused, the interference among BTSs is severe as more BTSs are using the same frequency and BTSs are closer to each other. Secondly, each BTS is costly to build and operate as it needs a considerable number of autonomous equipment, including its own cooling, back haul transportation, backup battery, monitoring system,etc. Although size and power of the electrical equipment is constantly being reduced, the supporting facilities of the BTS are not improving the same pace. Finally, because mobile users are moving from one place to another, the traffic managed by each BTS experiences considerable time fluctuations and, as a result, the average utilization rate of individual BTS is pretty low. However, these processing resources cannot be shared with other BTS. Thus all the BTS must be designed to handle the maximum traffic expected no matter the size of the average traffic. This implies a misuse of processing resources and unnecessary power consumption at idle times. These limitations have driven the evolution of these traditional architectures to more efficient configurations which we will now describe.

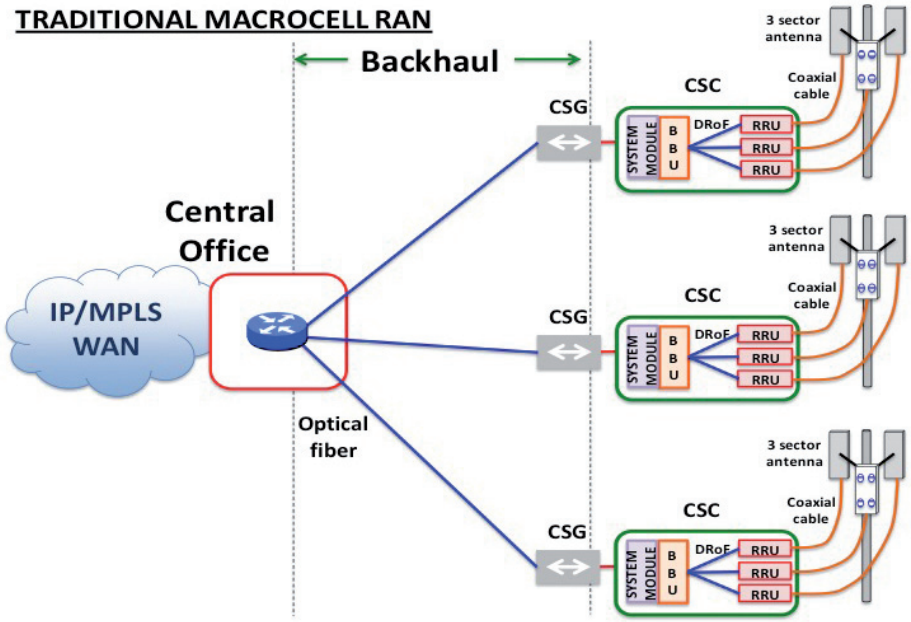

Figure 4. Architecture of a traditional RAN illustrating the backhaul segment.

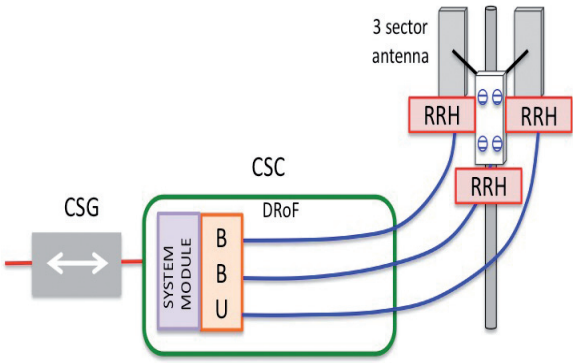

Figure 5. Basic layout of a distributed base station.

3. RAN and BTS Architecture evolution

3.1 Distributed Base Station architecture with traditional backhaul

The first evolution step is based on the concept of distributed BTS architecture. In this, the RRU, now RRH is separated from the RRH by optical fiber links as shown in figure 5.

Installing the RRH on the top of tower, close to the antenna, reduces the cable loss compared to the traditional base station where the RF signal has to travel through a long cable from the BTS CSC to the antenna at the top of power. The fiber link between RRH and BBU improves the flexibility in network planning and deployment as they

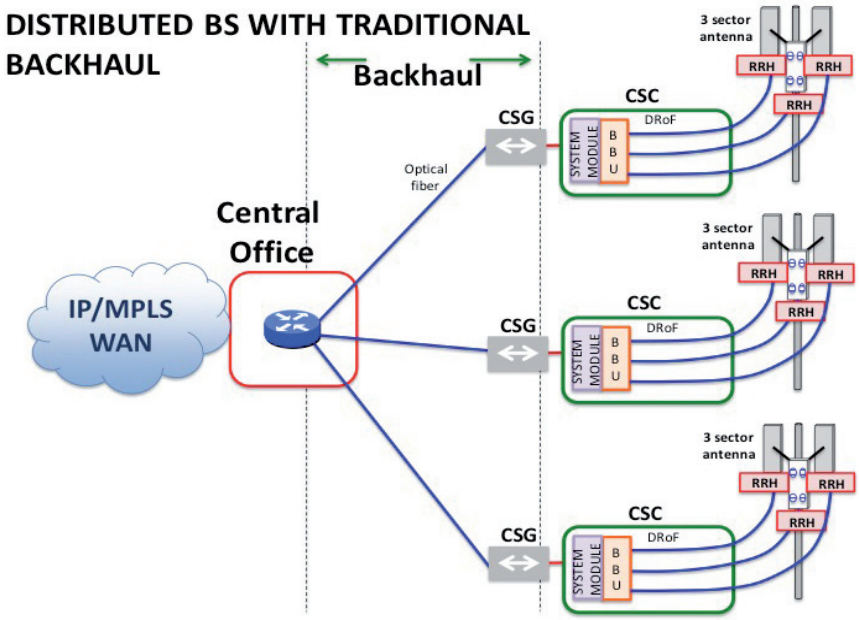

Figure 6. Architecture of a distributed base station RAN with traditional backhaul.

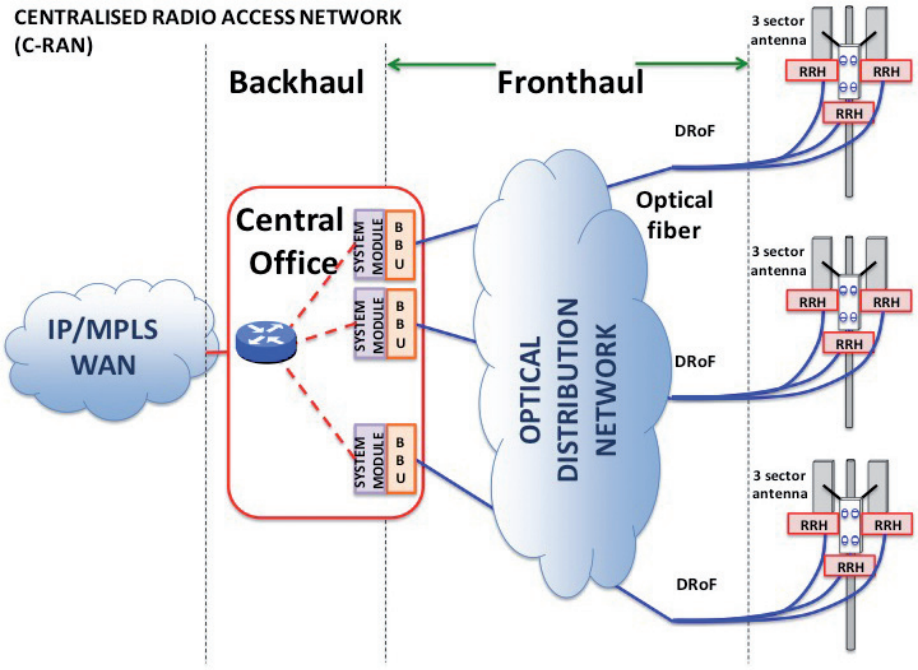

Figure 7. Architecture of a C-RAN showing the fronthaul and backhaul segments.

can be now placed at distances ranging from a few hundreds meters or a few kilometers away. This option is the one currently implemented in most modern base stations leading to a network configuration shown in figure 6.

Note that this network architecture still keeps a backhaul segment in between the central office and the BTS CSGs. This configuration, brings other additional advantages, like power saving but can result in increased operation (OPEX) and Capital (CAPEX) expenditure if the cell sites are not secured, as then IPSec protection is required.

3.2 Centralised RAN C-RAN

C-RAN, also known as Cloud RAN is an architecture evolution based on the distributed base station architecture described above . The basic layout of the architecture is illustrated in figure 7.

As it can be observed, the BBUs are pulled towards (in fact hosted at) the CCO. This leads to the novel concept of fronthaul segment, which is that part that connect the radiating elements with the now centralised BBUs. A backhaul segment is also present in between the BBUs and the connection node to the transport WAN. C-RAN combines many existing technology advances in wireless communication, optical transmission and IT technologies. For instance, it employs the latest CPRI standard, low cost CWDM/DWDM technology, or mmWave to allow the transmission of baseband signal over long distances to achieve large scale centralized base station deployment. It applies recent Data Center Network (DCN) technologies to allow low cost, high reliability, low latency and high bandwidth interconnect network in the BBU pool. It uses open platform and real-time virtualization technologies rooted in cloud computing to achieve dynamic shared resource allocation in the BBU pool and support of multi-vendor, multi-technology environment.

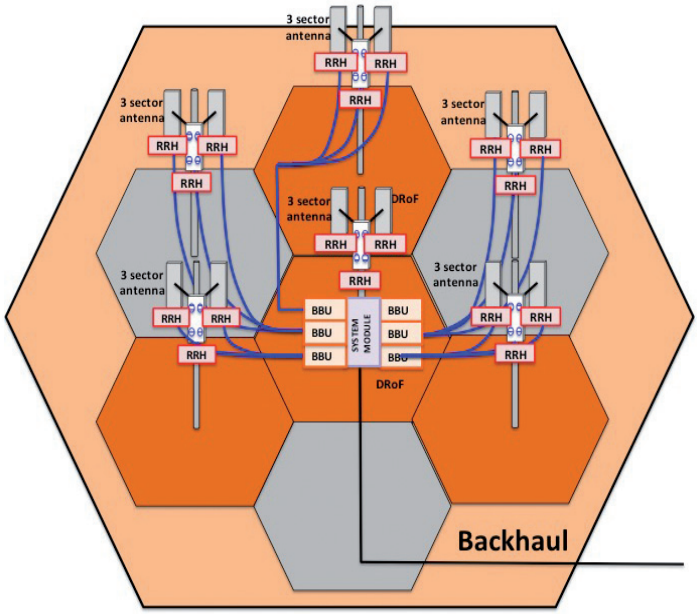

Figure 8. Illustration of the higher density coverage area of C-RAN.

The C-RAN architecture is characterized by several distinctive features as compared to the other cellular network architectures. In first place, as it builds upon large scale centralized deployment, it has the potential for allowing hundreds or even thousands of remote RRHs to be connected to a centralized BBU pool. This allows for a higher coverage density from a single CO as shown in figure 8 as compared to the case of a traditional BTS network architecture shown in figure 3.

C-RAN is conceived, in principle, to span maximum fiber link distances of up to 20 km for 4G (LTE/LTE-A) systems and 40-80 km for 3G (WCDMA/TD-SCDMA) and 2G (GSM/CDMA) systems. A second advantage of C-RAN is that it can provide native support to CoMP radio technologies. Since any BBU can fastly communicate at very high speed (10 Gb/s and above) and very low latency with any other hosted at the same pool then almost instantaneous coordination between different cells required for CoMP is guaranteed. Finally, the real-time virtualization capability based on open platform assures that the multi-vendor resources in the BBU pool can be flexibly and dynamically to base station software stacks (for example 4G/3G/2G function modules) according to network load.

4. Multicore Fiber link between the Central Office and the base Station Segment

4.1 Basic Configuration

The basic building block of the proposed architecture is a link between the CO and a single N-antenna sector based on a $(2N+1)$-core homogeneous MCF, which is shown in Fig. 9. In this work we only consider homogeneous MCFs since heterogeneous MCFs, which provide a different propagation characteristic per node preventing the time matched parallel transmission required for MIMO. Another possibility for SDM is the use of few mode fibers (FMFs), however this scheme brings in our opinion no relevant advantage since it would require complex modal injection and separation at the input and the output of the field, preventing a low-cost approach and furthermore, making it very difficult to control the coupling between propagation modes. Therefore, this alternative has been discarded in this paper.

The output power of a single CW laser (optical wavelength λ_D) is divided into N equal parts. Each one is modulated by a different signal, which can be either baseband I-Q in the case of CPRI or radiofrequency for a RoF approach. The figure illustrates the particular case of a multiple input multiple output (MIMO) transmission link, where each signal is then injected to each one of the N different cores employed for downstream transmission using subcarriers with the same RF frequency f_{RF1}. At the end of the L-km fiber link (antenna mast) each signal is detected by a separate receiver and processed by the RRH before being radiated. The link however is versatile enough to accommodate different RF signals centered at subcarriers with different RF frequencies in each core. Note that a single core is also employed to distribute the CW laser (optical wavelength λ_U) for upstream transmission and, possibly, a control and supervision channel. This CW signal is evenly divided between the N cores employed as a common optical carrier for upstream transmission where each of the N antennas receives its particular signal and modulates the common carrier after processing it at the RRH. The independent received channels are then sent to the CO. For interfacing the MCF to the external equipment, multicore fiber connectors (MCFCs) are considered.

4.2 Analog Link design

Each core supports, in essence, an analog radio over fiber, intermediate frequency (IF) or digital baseband link from the CO to the BS in downstream transmission and from the BS to the CO in upstream transmission. Ideally, for true parallel operation the cores in the MCF should be completely uncoupled. In practice, inter-core coupling must be taken into account in the design of each individual core link. For a standard analog link the performance is usually described in terms of the electrical carrier to noise ratio or CNR [8], [9]:

$$CNR = \frac{\left(m\Re P\right)^2/2}{\left\langle \Delta i_{shot}^2 \right\rangle + \left\langle \Delta i_{th}^2 \right\rangle + \left\langle \Delta i_{RIN}^2 \right\rangle + \left\langle \Delta i_{imd}^2 \right\rangle}, \quad (1)$$

where m is the modulation index, $\Re$ the detector responsivity, P the average optical power on the photodiode and $\langle \Delta i_{shot}^2 \rangle$, $\langle \Delta i_{th}^2 \rangle$, $\langle \Delta i_{RIN}^2 \rangle$, $\langle \Delta i_{imd}^2 \rangle$ the *RMS* powers associated to shot, thermal, relative intensity noises and the intermodulation distortion, respectively. For the pure noise sources:

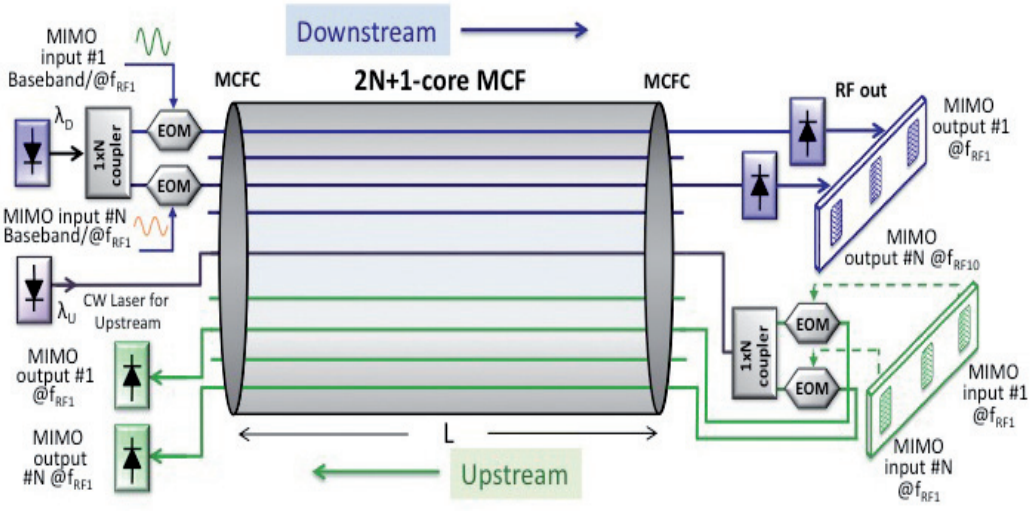

Figure 9. Link between CO and BS sector using a (2N+1)-core MCF.

ISSN 1889-8297/Waves - 2015 - year 7

$$\left\langle \Delta i_{shot}^2 \right\rangle = 2e\Re P\Delta f,$$
$$\left\langle \Delta i_{th}^2 \right\rangle = \frac{4k_B T F_n \Delta f}{R_L}, \quad (2)$$
$$\left\langle \Delta i_{RIN}^2 \right\rangle = RIN\left(\Re P\right)^2 \Delta f,$$

Where e is the electron charge, k_B the Boltzman constant, T the temperature, RIN the relative intensity noise of the laser, F_n and R_L represent the noise figure and the load resistor of the receiver, respectively, and deltaf the detector bandwidth. If inter-core crosstalk is taken into account, then (1) must be modified. For instance, the link equation for core "n" and low crosstalk values will be given by:

$$CNR_n = \frac{\left(m\Re P_n\right)^2/2}{\left\langle \Delta i_{shot,n}^2 \right\rangle + \left\langle \Delta i_{th,n}^2 \right\rangle + \left\langle \Delta i_{RIN,n}^2 \right\rangle + \left\langle \Delta i_{imd,n}^2 \right\rangle + \left\langle \Delta i_{XTALK,n}^2 \right\rangle} = \frac{1}{\frac{1}{CNR_{shot,n}} + \frac{1}{CNR_{th,n}} + \frac{1}{CNR_{RIN,n}} + \frac{1}{CNR_{imd,n}} + \frac{1}{CNR_{XTALK,n}}}, \quad (3)$$

where $\left\langle \Delta i_{XTALK,n}^2 \right\rangle$ is the *RMS* power associated to the equivalent noise due to crosstalk from all the cores $j \neq n$, P_n is the average optical power at the output of the n-th core and:

$$CNR_{u,n} = \frac{\left(m\Re P_n\right)^2/2}{\left\langle \Delta i_{u,n}^2 \right\rangle} \quad (4)$$

represents the carrier-to-noise ratio due to the particular noise source u, $u = \{shot, th, RIN, imd, XTALK\}$.

To compute the crosstalk contribution we need to know $|\Delta P_{n,k}|$, the value of the amplitude of the optical power fluctuations due to crosstalk from core k at the output of core n [10], [11]. The quotient between $|\Delta P_{n,k}|$ and mP_n is known as the amplitude crosstalk transfer function *XTTF*:

$$\left|XTTF_{n,k}(\omega)\right| = \left|\frac{\Delta P_{n,k}}{mP_n}\right|. \quad (5)$$

An empirical expression for its average and variance values has been derived in [10]:

$$\left\langle \left|XTTF_{n,k}(\omega)\right| \right\rangle = \left\langle \left|\frac{\Delta P_{n,k}}{mP_n}\right| \right\rangle = \frac{2\kappa^2 RL}{\beta D_{mn}} \sqrt{\left[0.31 + 0.69\,\mathrm{sinc}^2\left(\frac{\omega\left(\beta_{1,n} - \beta_{1,k}\right)L}{2}\right)\right]},$$
$$Var\left\{\left|XTTF_{n,k}(\omega)\right|\right\} = \left(\frac{2\kappa^2 RL}{\beta D_{nk}}\right)^2 \left[0.19 + 0.81\,\mathrm{sinc}^2\left(\frac{\omega\left(\beta_{1,n} - \beta_{1,k}\right)L}{2}\right)\right]. \quad (6)$$

In (6), ω is the signal angular frequency, κ is the coupling coefficient between cores n and k (a typical value range is 0.001 to 0.01 m^{-1}), R is the MCF curvature radius (a typical value ranges between 0.2 and 0.5 m), L is the MCF length (for typical access networks ranges between 2 and 25 km), $D_{n,k}$ is the separation between cores n and k (a typical value ranges between 35 and 45 m) and b is the propagation constant of the fundamental mode in cores n and k, which is assumed to be equal (a typical value ranges between 7-10 rad/ m). The parameter $d_{n,k} = \beta_{1,k} - \beta_{1,n} = 1/v_{g,n} - 1/v_{g,k}$ is the so-called skew per unit of length between cores n and k, and depends on the group velocities in both cores (a typical value is in the range of 0.01 and 0.1 ps/km).

The impact of intercore crosstalk can be neglected in the majority of access networks where front-haul optical links are below 10 km.

Now, since $|\Delta i_{n,k}| = \Re\,|\Delta P_{n,k}|$ it follows that $\Delta i^2_{n,k} = \Re^2|\Delta P_{n,k}|^2$ and therefore:

$$\frac{1}{CNR_{XTALK,n,k}} = \frac{2\left\langle \Delta i_{n,k}^2 \right\rangle}{\left(m\Re P_n\right)^2} = \frac{2\left\langle \left|\Delta P_{n,k}\right|^2 \right\rangle}{\left(mP_n\right)^2} = 2\left\langle \left|XTTF_{n,k}(\omega)\right|^2 \right\rangle. \quad (7)$$

The total crosstalk in core n is due to the contribution of the rest of the cores in the MCF:

$$\frac{1}{CNR_{XTALK,n}} = \sum_{k \neq n} \frac{1}{CNR_{XTALK,n,k}} = 2\sum_{k \neq n} \left\langle \left|XTTF_{n,k}(\omega)\right|^2 \right\rangle = \sum_{k \neq n} H_{n,k}. \quad (8)$$

To compute $H_{n,k}$, we make use of (6):

$$H_{n,k} = 2\left\langle \left|XTTF_{n,k}(\omega)\right|^2 \right\rangle = 2\left\{Var\left\{\left|XTTF_{n,k}(\omega)\right|\right\} + \left[\left\langle \left|XTTF_{n,k}(\omega)\right| \right\rangle\right]^2\right\} = \left(\frac{2\kappa^2 RL}{\beta D_{nk}}\right)^2 \left[1 + 3\,\mathrm{sinc}^2\left(\frac{\omega\left(\beta_{1,n} - \beta_{1,k}\right)L}{2}\right)\right]. \quad (9)$$

For the evaluation of (8) it is customary to take an upper bound corresponding to the worst case [7], [11], [12], which in typical hexagonal 7- and 19-core MCFs corresponds to the central core ($n = 1$). For the case of a 7-core MCF, the distance D between the central and surrounding cores is the same, hence, if we assume an equal skew per unit of length between the central and the surrounding cores we have $H_{1,k} = H_1$, $\forall k$. Since only half of the cores contribute to upstream/downstream transmission then:

$$\left.\frac{1}{CNR_{XTALK}}\right|_{7C-MCF} = 3H_1. \quad (10)$$

For the case of a 19-core MCF, if the 6 internal surrounding cores are at a distance D from the central core, there are other 6 at a distance $2D$ and another 6 at a distance $\sqrt{3}D$. Thus we have:

$$\left.\frac{1}{CNR_{XTALK}}\right|_{19C-MCF} = \frac{19H_1}{4}. \quad (11)$$

Introducing (10) or (11) in (3) renders the complete CNR expression that takes into account the impact of the inter-core crosstalk.

Fig. 10 shows the value of $1/CNR_{XTALK}$ as a function of the modulating frequency taking the link length L as a parameter, for a standard 19-core MCF with $\kappa = 0.01$ m^{-1}, $R = 0.5$ m, $D_{n,k} = 44$ μm, $\beta = 6$ rad/μm and $d_{n,k} = 0.03$ ps/km.

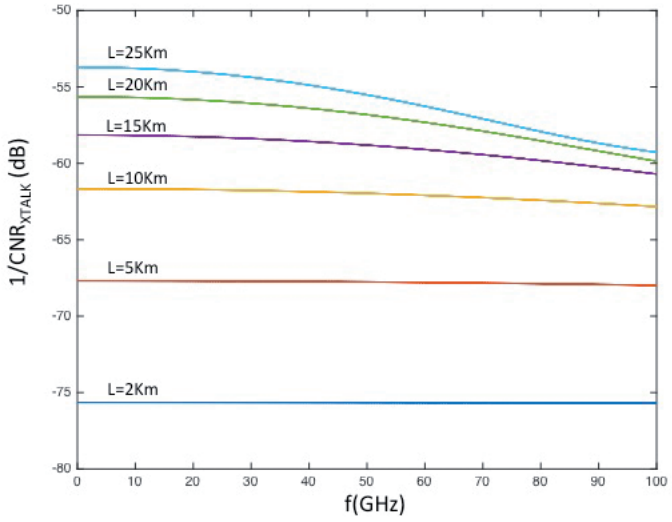

Figure 10. $1/CNR_{XTALK}$ as a function of the modulating frequency taking the link length L as a parameter, for a standard 19-core MCF with $\kappa = 0.01$ m^{-1}, $R = 0.5$ m, $D_{n,k} = 44$ μm, $\beta = 6$ rad/μm and $d_{n,k} = 0.03$ ps/km.

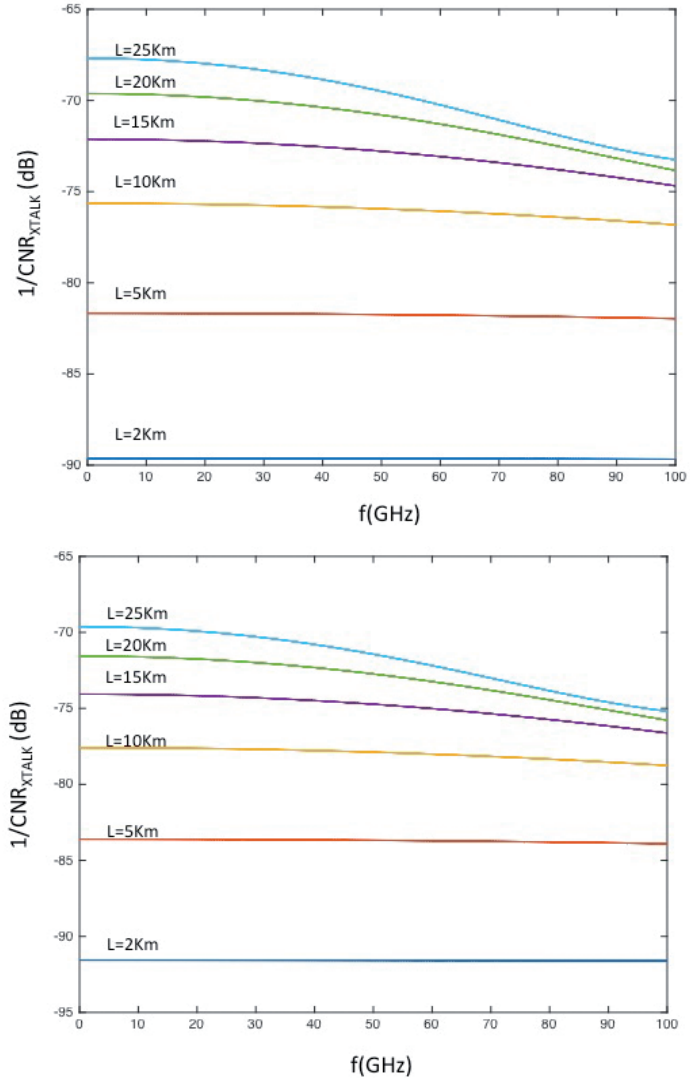

Figure 11. $1/CNR_{XTALK}$ as a function of frequency taking the link length L as a parameter, for a standard 19-core MCF. Top: $\kappa = 0.002$ m^{-1}, $R = 0.5$ m, $D_{n,k} = 44$ μm, $\beta = 6$ rad/μm and $d_{n,k} = 0.03$ ps/km. Bottom: $\kappa = 0.01$ m^{-1}, $R = 0.2$ m, $D_{n,k} = 44$ μm, $\beta = 6$ rad/μm and $d_{n,k} = 0.03$ ps/km.

Relevant electrical crosstalk levels (comparable to other noise sources if >-65 dB [7]) can be achieved for moderate link distances (>10 km). For short RAM links, below 10 km, the impact of crosstalk can be safely considered as negligible as compared to other noise sources.

However, these levels can be reduced either by reducing the values of the coupling coefficients between cores or by reducing the value of the critical bending radius. To achieve this, trench-type MCFs have been proposed and demonstrated [11]. Fig. 11 shows the value of $1/CNR_{XTALK}$ as a function of frequency taking the link length L as a parameter, for the same case as in Fig. 2 when the coupling coefficient is reduced from $\kappa = 0.01$ m^{-1} to $\kappa = 0.002$ m^{-1} (left) and when the critical bending radius is reduced from $R = 0.5$ to 0.2 m (right).

In both cases and even for link lengths over 10 km the crosstalk levels are below <-70 dB, which in practice is a negligible value. For links above 10 km, the crosstalk performance must be considered but its behavior can be quite frequency dependent as recently reported in [10], this is a consequence of the increase of the skew $d_{n,k}L$ between coupled cores. This feature is slightly apparent and also depends on the value of the skew per unit length value, which can range from 0.01 to 0.1 ps/km.

From the results obtained by simulation it is expected that inter-core crosstalk noise will only be significant if the link length is >10 km and if a non-optimized MCF design is employed. In practice, since around a 96% of the access network links in Europe are below 10 km, this means that the impact of crosstalk can be neglected in most cases and link design can be carried independently core by core.

5. Multicore Fiber based CRAN Front-Haul Architectures

5.1 Radio over Fiber Operation

The single CO-BS SDM-based link described in the previous section can serve as the basic sector connection for RoF access networks. Fig. 12 shows a representative C-RAN distribution architecture where the CO is connected to each one of the sectors conforming the different BSs by means of $2N$+1-core MCFs, (N cores for downstream transmission and N cores for upstream transmission). The i-th input core to/from sector j in BS_k is labeled as s_i^{kj}, as shown in the expanded picture of a MCF link displayed in the lower part of Fig. 12. A centralized switch placed in the CO provides the dynamic mapping of/to downstream/upstream subcarrier channels and bands to/from the spatial ports. The fabric includes an internal electronic core where SDN switching is performed prior to the modulation of the λ_D laser in downstream and after detection of the λ_U signal in upstream.

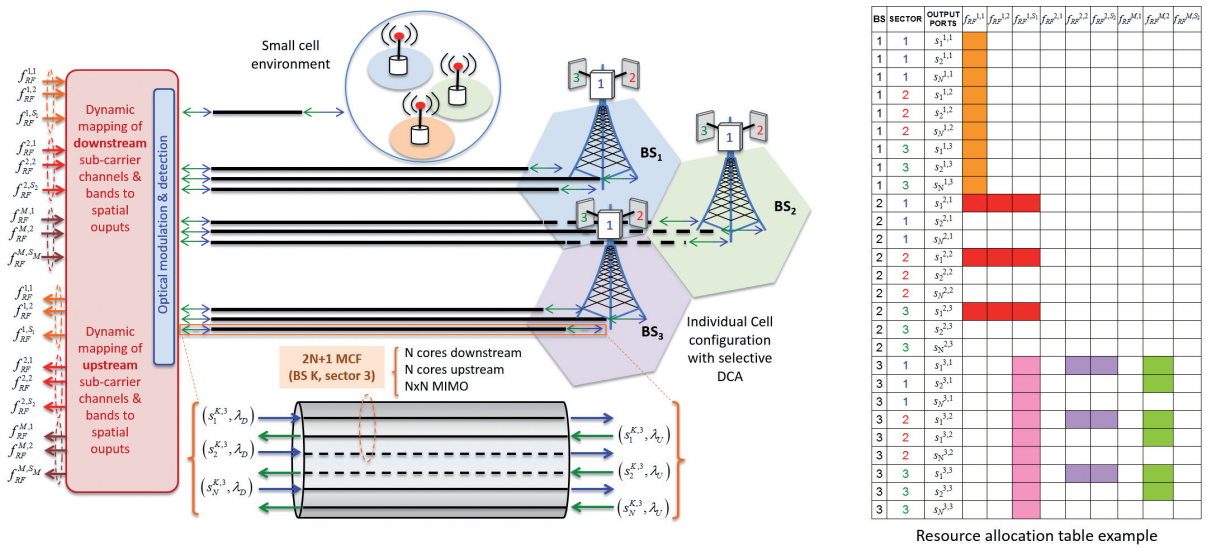

Figure 12. (Left) MCF-based C-RAN configuration for RoF operation. (Right) Example of a resource allocation table.

The spatial diversity available at the CO output provides several advantages. First, each sector within a given BS can be independently addressed and software-defined configured with a MCF having a similar outer diameter as a SMF-28, thus avoiding fiber bundling. Second, resource allocation can be implemented electronically enabling both carrier aggregation and MIMO operation. Third, the number of MIMO radiators in a given sector can be independently and dynamically set from 1 to N at the CO, enabling, for instance, CoMP from adjacent sectors in neighboring BSs.

As an example, the resource allocation table on Fig. 12 shows a representative switching configuration where BS_1 provides capacity expansion by using NxN MIMO over only one frequency allocated in band 1 ($f_{RF}^{1,1}$); BS_2 provides capacity expansion by carrier aggregation using three carriers in band 1 ($f_{RF}^{1,1}, f_{RF}^{1,2}, f_{RF}^{1,S1}$) in the three sectors and only one radiator per sector (no MIMO); while BS_3 features capacity expansion by using NxN MIMO in band 1 ($f_{RF}^{1,S1}$), carrier aggregation in band 2 ($f_{RF}F^{2,2}, f_{RF}^{2,S2}$) and 2x2 MIMO in band M ($f_{RF}^{M,2}$).

5.2 Digitized Radio over Fiber Operation

The Fig. 13 shows the proposed configuration of a C-RAN architecture based on the CO-BS basic link applied to DRoF operation. In this case, the input (downstream signal)/output (upstream signal) to/from the electronic switch placed at the CO corresponds to a BBU pool where a series of virtual BBUs are defined by software to service BS_1 to BS_M. Each virtual BBUm, with $m = 1$ to M, can be reconfigured to allocate different capacities dynamically. Resources are allocated to the virtual BBUs by an overall manager, and each virtual BBU is directly tied to specific cores of a given MCF.

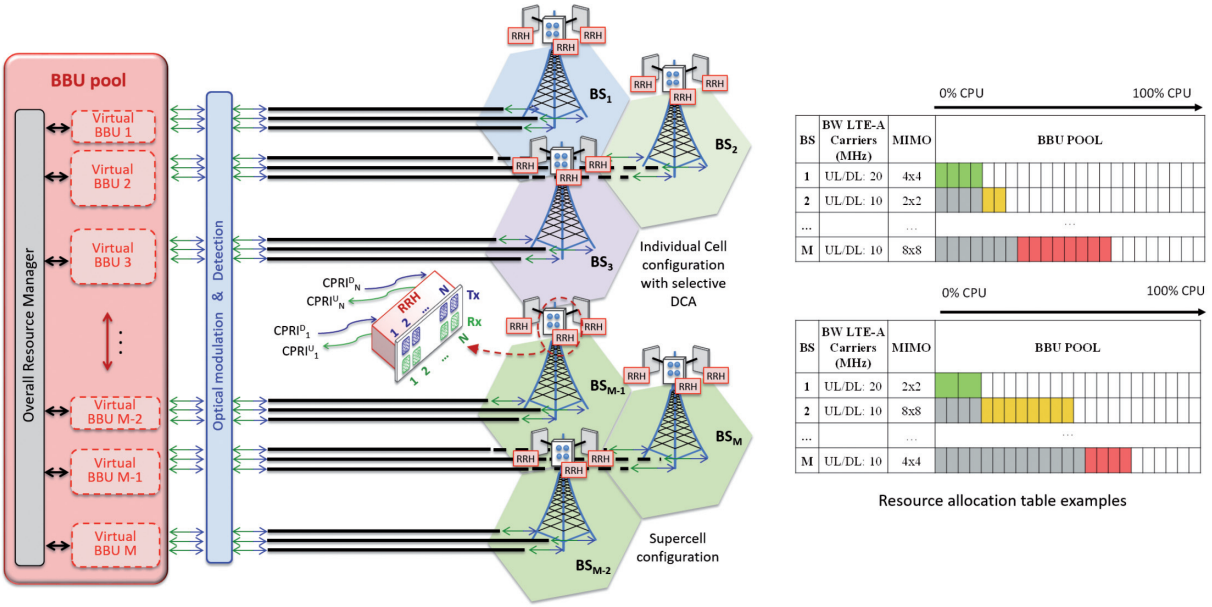

Figure 13. (Left) MCF-based C-RAN configuration for DRoF operation. (Right) Example of a resource allocation table.

The resource allocation table illustrated in Fig. 13 shows two representative examples of resource reconfigurations given in a DRoF scenario. In both cases we assume equal capacity/sector at each BS. In the upper table we illustrate the case of carrier aggregation over multi-band non-contiguous (800-900 MHz) 10+10 MHz for LTE-A using different configurations of MIMO. If only one antenna is active, the CPRI bit rate is 1.536 Gb/s that is actually illustrated as a basic CPU unit. For instance, BS_1 and BS_2 implement independent 4x4 and 2x2 MIMO with an overall capacity per sector of 6.14 and 3.07 Gb/s, respectively. On the other hand, the set conformed by BS_{M-2}, BS_{M-1} and BS_M implements a supercell with 8x8 MIMO and an overall capacity per sector of 12.28 Gb/s. The cumulative capacity employed in terms of % of CPU usage of the BBU pool is illustrated in grey.

The lower table illustrates a situation where the capacity is being reassigned. Here single-band non-contiguous (900 MHz) 5+5 MHz for LTE-A is supported using different configurations of MIMO. If only one antenna is active, the CPRI bit-rate is 0.768 Gb/s that is illustrated as a basic unit.

Bit rates are kept to 1.536 Gb/s for the cores feeding BS_1 and its overall capacity per sector is now 3.07 Gb/s while the number of radiators is changed from 4 to 2; for BS_2 the number of radiators changes from 1 to 8, the bit rate per core is 0.768 Gb/s while the overall capacity per sector is increased to 6.14 Gb/s. Finally, the supercell implemented by BS_{M-2}, BS_{M-1} and BS_M provides a capacity of 3.07 Gb/s per sector.

6. MCF C-RAN integration with PONs

The proposed MCF-based RAN architecture brings an additional advantage since due to the spatial diversity provided by the MCFs it can easily integrate a passive optical network architecture. The most straightforward configuration is that shown in Fig. 14. Here, using *2N*-2 cores for the downstream/upstream MIMO transmission, and 1 core for the upstream CW laser distribution, leaves two free cores to support the downstream and upstream transmission required by a PON. Each one of these can carry digital baseband information using the regulated wavelength pertaining to each propagation direction. In the configuration displayed in Fig. 7 the downstrean/upstream cores are connected to 1xM couplers for further power division/sum respectively, but they cold be directly tied to a final optical network unit (ONU).

The results obtained in Section 4 indicate that uniform (and negligible) spectral behavior regarding crosstalk should be expected in most practical situations in the spectral region spanning from baseband to 10 GHz, therefore this configuration should be, in principle capable of supporting any of the current PON standards (1 & 10 GPON). Furthermore, as the transmission in each core is compatible with a WDM overlay, it will also be capable of supporting emerging WPON standards.

As an example, Table 1 shows possible configurations where C-RAN with MIMO, control channels and PON are directly integrated for different MCF models. For each case the maximum MIMO diversity is displayed in the second column.

MCF Design	MIMO	PON	Control
7-Core Homogeneous	2x2	2	1
12-Core Homogeneous	3x3	2	1
19-Core Homogeneous	8x8	2	1
36-Core Homogeneous	16x16	2	1

Table 1. MIMO C-RAN AND PON INTEGRATION OPTIONS FOR DIFFERENT MCF DESIGNS.

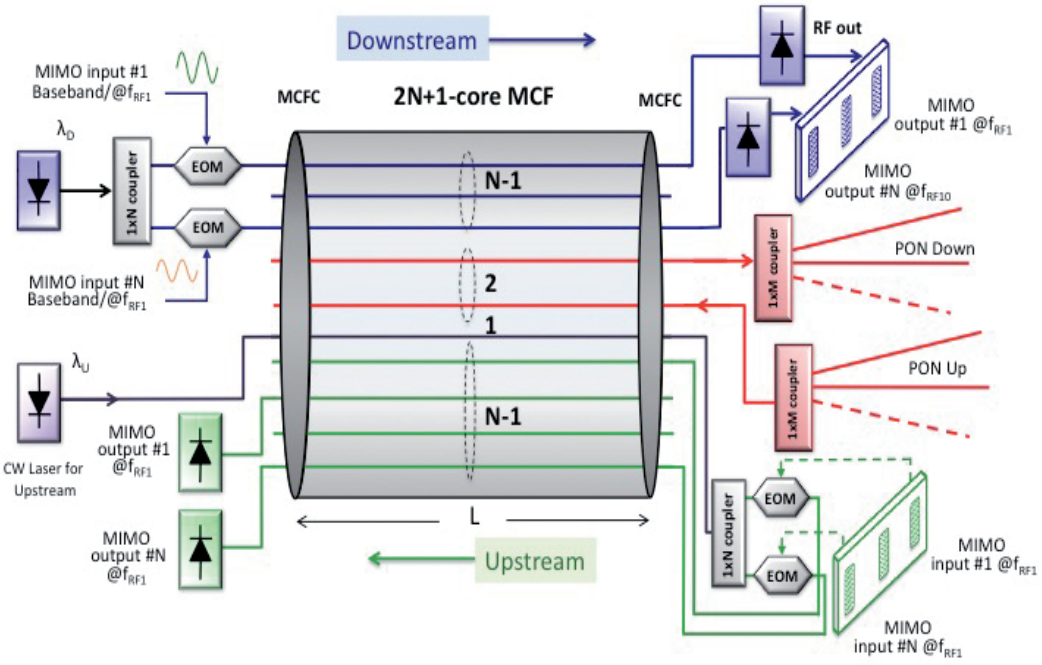

Figure 14. MCF-based C-RAN configuration incorporating PON integration.

7. Summary and Conclusions

The use of MCFs to support C-RAN architectures can help to address their main present and future challenges through the exploitation of spatial division multiplexing. This novel approach allows SDN and NFV and is compatible with both WDM and PON overlay expansion. SDN and NFV implementation can be achieved by exploiting the fact that both in the DRoF and RoF approaches the traffic and capacity characteristics of each sector in each BS can be reconfigured by software in the electrical domain through an overall resources manager located in the electronic switch (shown in figure 13). Furthermore, the proposed architecture is potentially integrable with MCF-based solutions for metro networks if architecture on demand (AoD) gateway nodes [13] are introduced at the CO. A possible solution would require spatial switching and could be built upon the process described in [14].

References

[1] C. Lim, A. Nirmalathas, M. Bakaul, P. Gamage, K.-L. Lee, Y. Yang, D. Novak, and R. Waterhouse, "Fiber-Wireless Networks and Subsystem Technologies," J. Lightwave Technol, 28,. 390 –405, (2010).

[2] P. Chanclou et al "Optical Fiber Solution for Mobile Fronthaul to Achieve Cloud Radio Access Network", in Future Network & Mobile Summit 2013 Conference Proceedings, (2013).

[3] A. Pizzinat et al., "Things you should know about Fronthaul," J. Lightwave Technol., vol. 33, pp. 1077-1083, 2015.

[4] A. Saadani et al., "Digital Radio over Fiber for LTE-Advanced: Opportunities and Challenges," in Proc. ONDM 2013, Brest, France, 2013, pp. 194.

[5] J. E. Mitchell, "Integrated wireless backhaul over optical access networks," IEEE J. Lightwave Technol., vol. 32, pp. 3373-3382, 2014.

[6] C. Liu et al., "Key Microwave-Photonics Technologies for Next-Generation Cloud-Based Radio Access Networks," IEEE J. Lightwave Technol., vol. 32, pp. 3452-3460, 2014.

[7] M. Koshiba, "Design aspects of multicore optical fibers for high-capacity Long-Haul transmission," in Proc. IEEE Top. Meeting MWP 14, Sapporo, Japan, 2014, pp. 318.

[8] J. Capmany and D. Novak, "Microwave photonics combines two worlds," Nat. Photonics, vol. 1, no. 6, pp. 319-330, 2007.

[9] J. Yao, "Microwave photonics," IEEE J. Lightwave Technol., vol. 27, no. 3, pp. 314-335, 2009.

[10] R.S. Luis, B.J. Puttnam, A. V. Cartaxo, W. Klaus, J.M. Mendinueta, Y. Awaji, N. Wada, T. NNakanishi, T. Hayashi and T. Sasasaki, "Time and modulation frequency dependence of crosstalk in homogeneous multi-core fibers," IEEE J. Lightwave Technol., in press.

[11] T. Hayashi, T. Taru, O. Shimakawa, T. Sasaki, and E. Sasaoka, "Design and fabrication of ultra-low crosstalk and low-loss multi-core fiber," Opt. Express, vol. 19, pp. 16576-16592, 2011.

[12] M. Koshiba, K. Saitoh, K. Takenaga, and S. Matsuo, "Multi-core fiber design and analysis: coupled-mode theory and coupled-power theory," Opt. Express, vol. 19, no. 26, p. B102, Dec. 2011

[13] N. Amaya et al., "Software defined networking over space division multiplexing optical networks: features, benefits and experimental demonstration," Opt. Express, vol. 22, pp. 3638-3647, 2014.

[14] N. Amaya, et al., "Fully-elastic multi-granular network with space/frequency/time switching using multi-core fibres and programmable optical nodes," Opt. Express, vol. 21, pp. 8865-8872, 2013.

Biographies

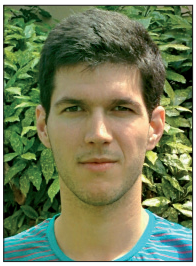

Jose Manuel Galve was born in Valencia, Spain, on September 23, 1991. He received the Ingeniero de Telecomunicación degree from the Universitat Politècnica de València (UPV), València, Spain in 2014. Since 2014, he is a Ph.D. student at the Optical and Quantum Communications Group, UPV. He works on the design of space division multiplexed fronthaul architectures for C-RANs.

Ivana Gasulla received the M. Sc. degree in Telecommunications Engineering and the Ph.D. degree from the Universidad Politecnica de Valencia (UPV), Spain, respectively, in 2005 and 2008. Her PhD thesis was recognized with the IEEE/LEOS Graduate Student Fellowship Award. From 2005 to 2011, she was working at the ITEAM Research Institute at UPV. After being awarded a Fulbright Post-Doctoral Fellowship, she carried out research at Stanford University on spatial multiplexing in multimode optical fibers during 2012 and 2013. In 2014 she joined again ITEAM Research Institute at UPV where she is now a Ramón y Cajal Postdoctoral research Fellow**.** Her research interests are mainly focused on microwave photonics, and Space Division multiplexing. Dr. Gasulla is a member of the Technical Program Committee of the European Conference on Optical Communications (ECOC).

Salvador Sales is Professor at the Departamento de Comunicaciones, Universidad Politécnica de Valencia, SPAIN. He is also working in the ITEAM Research Institute. He received the degree of Ingeniero de Telecomunicación and the Ph.D. in Telecomunicación from the Universidad Politécnica de Valencia. He is currently the coordinator of the Ph.D. Telecomunicación students of the Universidad Politécnica de Valencia. He has been Faculty Vicedean of the UPVLC in 1998 and Deputy Director of the Departamento de Comunicaciones in 2004-2008. He received the Annual Award of the Spanish Telecommunication Engineering Asociation to the best PhD. on optical communications. He is co-author of more than 80 journal papers and 150 international conferences. He has been collab-

orating and leading some national and European research projects since 1997. His main research interests include optoelectronic signal processing for optronic and microwave systems, optical delay lines, fibre Bragg gratings, WDM and SCM ligthwave systems and semiconductor optical amplifiers.

José Capmany was born in Madrid, Spain, on December 15 1962. He received the Ingeniero de Telecomunicacion degree from the Universidad Politécnica de Madrid (UPM) in 1987 and the Licenciado en Ciencias Físicas in 2009 from UNED. He holds a PhD in Electrical Engineering from UPM and a PhD in Quantum Physics from the Universidad de Vigo. Since 1991 he is with the Departamento de Comunicaciones, Universidad Politecnica de Valencia (UPV), where he started the activities on optical communications and photonics, founding the Optical Communications Group (www.gco.upv.es). He has been an Associate Professor from 1992 to 1996, and Full Professor in optical communications, systems, and networks since 1996. In parallel, he has been Telecommunications Engineering Faculty Vice-Dean from 1991 to 1996, and Deputy Head of the Communications Department since 1996. Since 2002, he is the Director of the ITEAM Research Institute, Universidad Politécnica de Valencia. His research activities and interests cover a wide range of subjects related to optical communications including optical signal processing, ring resonators, fiber gratings, RF filters, SCM, WDM, and CDMA transmission, wavelength conversion, optical bistability and more recently quantum cryptography and quantum information processing using photonics. He has published over 470 papers in international refereed journals and conferences and has been a member of the Technical Program Committees of the European Conference on Optical Communications (ECOC), the Optical Fiber Conference (OFC). Professor Capmany has also carried out activities related to professional bodies and is the Founder and current Chairman of the PS Spanish Chapter, member of IEEE PS BoG (2010-2012), and a Fellow of the Optical Society of America (OSA). Professor Capmany is the recipient of King James I Prize on Novel Technologies, the highest scientific distinction in Spain, in recognition to his outstanding contributions to the field of microwave photonics, the Extraordinary Engineering Doctorate Prize of the Universidad Politécnica de Madrid and the Extraordinary Physics Laurea Prize from UNED. He is an associate Editor of IEEE Photonics Technology Letters.